JTTEE5 14:384-390
DOI: 10.1361/105996305X59378
1059-9630/$19.00 © ASM International

Peer Reviewed

Evaluation of Corrosion and Wear Resistance of Hard Cermet Coatings Sprayed by Using an Improved HVOF Process

Y. Ishikawa, J. Kawakita, S. Osawa, T. Itsukaichi, Y. Sakamoto, M. Takaya, and S. Kuroda

(Submitted February 18, 2004; in revised form September 7, 2004)

Research for alternatives of hard chrome plating has been widely carried out in the world. High-velocity oxygen-fuel (HVOF)-sprayed cermet coating is one of such alternative candidates. Depending on the cermet powder for spraying, however, sometimes the density of the sprayed coatings is not sufficient for desired corrosion resistance. A gas-shroud (GS) attachment for use with commercial HVOF, which is effective in suppressing oxidation of sprayed particles while raising the velocity of sprayed particles, has been developed. The GS-HVOF spray has been successfully applied to corrosion resistant alloys such as HastelloyC. In this study, a WC cermet system with corrosion and wear resistance was sprayed using a gas-shroud attachment. Porosity in the coatings was observed by the microscopic observation of cross sections. Corrosion and wear resistance was evaluated by alternating current corrosion monitoring in artificial seawater and abrasive wear-tester, respectively. Coatings deposited by the gas-shroud HVOF were superior in terms of both corrosion and wear resistance to coatings formed by the conventional HVOF. The density of the sprayed coatings was improved using the gas-shroud attachment, resulting in superior corrosion and wear resistance.

Keywords gas shroud, high density, high-velocity oxygen-fuel, wear property

1. Introduction

Hard chrome plating is widely used to protect a broad range of mechanical components from corrosion and wear. However, hexavalent chromium associated with the chrome plating process can be detrimental to the environment and the operator's health. Therefore, research for alternatives to chrome plating has been widely carried out especially in Europe and America (Ref 1, 2). High-velocity oxygen-fueled (HVOF)-sprayed cermet coating is one alternative candidate.

The HVOF process owes both its heat source and acceleration force to a supersonic jet flame made from high-pressured mixture of oxygen and fuel. This technique enables us to obtain sprayed particles with a speed over 500 m/s and with a temperature up to around 2000 °C. When compared with other conventional methods such as plasma spraying, HVOF sprayed particles possess higher speed with lower temperature. Such particles impinge on to a target substrate often in the semimolten state and pile up to form coatings. Dense coatings with comparatively small change in material properties can be fabricated with this process (Ref 3).

However, there are some problems on coating preparation by HVOF thermal spraying. For some cermet powders, it is difficult to make a dense coating by this method. Density of coating is very important for impermeable anticorrosion coating in the film preparation. When one intends to decrease the porosity to make dense sprayed coatings by usual HVOF thermal spraying equipment, it is necessary to increase the combustion power, which tends to increase the degree of oxidation of the sprayed coatings. The increase of oxidation can be a reason of lowering of wear and corrosion resistance of the sprayed coatings.

It is well known that the flight velocity of sprayed particles is a function of the combustion pressure whereas the temperature of in-flight particles correlates to the fuel/oxygen ratio (Ref 4). Therefore, we have developed a gas-shroud attachment for HVOF (Fig. 1), with which it is possible to suppress oxidation of sprayed particles while raising their velocity.

The objective of this paper was to make dense coatings of WC/20 mass% Cr_3C_2/7 mass% Ni cermet, which is expected to have high wear as well as corrosion resistance. This cermet coating is widely used as wear-resistant coating for papermaking rollerss in Japan. Density of coatings was determined by cross-sectional observation. Wear resistance was evaluated by the Suga type wear-tester. Corrosion resistance was evaluated by alternating current (ac) impedance corrosion monitor in artificial seawater.

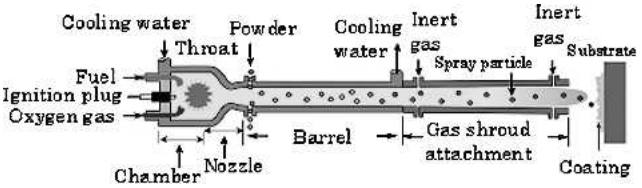

Fig. 1 Schematic representation of HVOF with the gas shroud attachment

Y. Ishikawa, J. Kawakita, and **S. Kuroda,** National Institution for Material Science, Thermal Spray Group, 1-2-1, Sengen, Tsukuba, Ibaraki 305-0047, Japan; **S. Osawa** and **T. Itsukaichi,** Fujimi Incorporated, 5-82-28, Kagamihigasi-tyo, Kagamihara, Gifu 509-0103, Japan; and **Y. Sakamoto** and **M. Takaya,** Chiba Institute of Technology, 2-17-1, Tsudanum, Narashino, Chiba 275-0016, Japan. Contact e-mail: Ishikawa.Yasunari@nims.go.jp

2. Experimental Method

2.1 Powder Characteristics and Spray Condition

Coatings were prepared with a HVOF thermal spray apparatus (JP5000, TAFA Co., Concord, NH), which uses kerosene and oxygen to generate a supersonic combustion flame. The cermet powder with size distribution from 15-53 μm (WC/20% Cr_3C_2/7% Ni, SURPREX W2007L, Fujimi Inc., Gifu, Japan) was used as the feedstock (Table 1).

The advanced HVOF equipment with a gas shroud shown in Fig. 1, which can introduce inert gas, was used in some flame conditions (Table 2). This equipment enables us to obtain three effects as follows: (1) decrease of spray particles' in-flight temperature, (2) suppression of sprayed particles' oxidation, and (3) increase of spray particles' in-flight velocity.

The substrate was JIS SS400 low carbon steel plate (5 × 50 × 100 mm), and its surface was blasted by alumina grit and degreased by ultrasonic cleaning in acetone. Table 1 shows the powder's chemical composition.

The basic operating conditions are listed in Table 2. The nitrogen flow rate at the upstream inlet of the shroud was 2500 l/min and the flow rate at the downstream inlet was 450 l/min. Thickness of all the coatings was aimed at 200 μm. Table 3 shows detailed spraying conditions and combustion pressure Pc used in the experiment. F/O is the fuel to oxygen ratio, where F/O = 1 corresponds to the stoichiometoric mixture ratio for complete combustion. Pc is the combustion pressure measured in the combustion chamber. Thermal spraying condition without gas shroud is from A to E. As it goes from A to E, the flame becomes more fuel rich from the oxidizing flame. The thermal spraying condition with gas shroud is from F to H. As it goes from F to H, combustion pressure increased.

2.2 Characterization of Sprayed Particles

We measured in-flight velocity and temperature of sprayed particles by the in-flight thermal sprayed particle analyzer (DPV-2000, TECNAR Co., Canada). Its principle and mechanism are described in detail elsewhere (Ref 5). This equipment utilizes the thermal radiation from the in-flight sprayed particles. The image of a hot particle is formed on a pair of vertical slits by means of a lens. Temperature is determined by the two-color pyrometry.

Table 1 Composition of the feedstock powder SURPREX W 2007L

Measurement	Value
Spray material, mass%	WC/20% Cr_3C_2/7% Ni
Particle size, μm	−53+15
Apparent density, g/cm^3	3.99
Particle size distribution, μm (mass%)	+53% (1.1)
	+45 (9.5)
	+32 (42.7)
	−20 (11.0)
	−15 (2.2)
	−10 (0.1)
Chemical composition, mass%	bal W
	18 Cr
	6.9 Ni
	7.2 C
	0.09 Fe

Velocity is determined by dividing the distance between the two slits (160 μm) by the time between two radiation signals detected when the image of one particle passes in front of the slits.

2.3 Characterization of Coatings Structure and Phases

The cross section of the coated specimens was observed by an optical microscope (Olympus, BX60M, Japan). The cross section was prepared by embedding the coated specimen into a thermosetting epoxy resin by an automatic mounting press (Buehler, SIMPLIMET2000, USA), followed by grinding and polishing. The crystal structure of powder and coatings is characterized by the x-ray diffraction measurement with Cu K_α radiation (RINT 2500, Rigaku Co., Japan). Even though specimens were prepared under all the spraying conditions (A-H), selected representative results will be reported for the evaluation below.

2.4 Corrosion Monitoring Test

Corrosion resistance, corrosion potential, etc. were evaluated by using an ac impedance corrosion monitor (Model CT-5, Riken Denshi, Japan) in artificial seawater (Fig. 2). The experimental procedure of this method is as follows.

A SS400 steel specimen coated by HVOF spraying of cermet was cut into square pieces with one side of 25 mm. A stainless steel rod was connected to the back surface of the substrate plate by spot welding. The sprayed area of 200 mm^2 was left exposed, and the rest of the specimen surface was insulated with silicone resin. This specimen was immersed in artificial seawater at room temperature for 72 h. During immersion, corrosion resistance and corrosion potential of the coated specimen in artificial seawater were measured continuously by using the corrosion monitor in every 30 min. The coating surface was observed by the optical microscope after the test. The composition of the artificial seawater is NaCl: 2.45%, MgCl: 1.11%, Na_2SO_4: 0.41%, $CaCl_2$: 0.15%, KCl: 0.07%.

2.5 Vickers Hardness Test

The hardness of coatings was measured using the micro Vickers

Table 2 Basic operating conditions

Parameter	Unit	Value
Barrel length	mm	150
Powder feed rate	g/min	70
Torch velocity	mm/s	700
Spray distance	mm	300
Powder feed gas	…	nitrogen
Coating thickness	μm	200

Table 3 Spraying conditions

Condition	Fuel, l/min	Oxygen, l/min	F/O	P_c, MPa
A	0.32	897	0.73	0.63
B	0.38	991	0.78	0.72
C	0.41	944	0.88	0.72
D	0.44	920	0.98	0.72
E	0.44	826	1.09	0.67
F	0.44	826	1.09	0.67
G	0.47	885	1.09	0.72
H	0.50	944	1.09	0.77

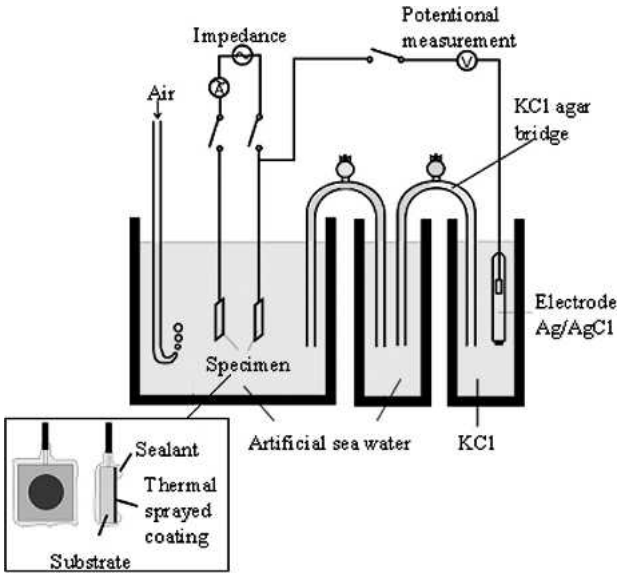

Fig. 2 Schematic representation of corrosion monitoring tester

hardness tester (MVK-E, Akashi Co., Japan). Microhardness measurements of the coatings were made with a 300 gf load/15 s. The results are reported as the average values of five indents, which were made along the midplane of polished cross section of coatings.

2.6 Wear Test

Wear test of the coatings was performed using a Suga-type reciprocation wear tester (two body abrasive wear tester). As shown in Fig. 3, this tester uses a wear ring of 12 mm width and 50 mm diameter, which is rolled with an abrasive paper of SiC. A cermet coated flat specimen was cut into pieces 50 mm square and placed on top of the abrasive ring. Under the loading of 30 N between the abrasive ring and the specimen, the specimen reciprocates in 30 mm once, and then the wear ring is rotated by 0.9° to bring a fresh surface of the abrasive paper into contact with the specimen surface. This cycle is repeated for the desired number of cycles. The wear amount of specimen was measured in every 360° revolution of the abrasive ring. Scanning electron microscopy (SEM) was used to study the worn surfaces and wear debris.

3. Results and Discussion

3.1 Characterization of Sprayed Particles

Figure 4 shows the spray particles' velocity and temperature in flight at each condition. Without the gas shroud (A-E), spray particles' in-flight velocity increased from 680 to 780 m/s as the combustion pressure Pc, shown in Table 3, increased from 0.63 to 0.72 MPa. This is as expected from the past research (Ref 4, 5). On the contrary, the surface temperature of the particles almost remained constant around 1950 °C, even though the fuel/oxygen ratio changed from 0.73 to 1.09. Such tendency of spray particles' in-flight temperature was not in agreement with the past research (Ref 4, 5). With the gas shroud mounted conditions

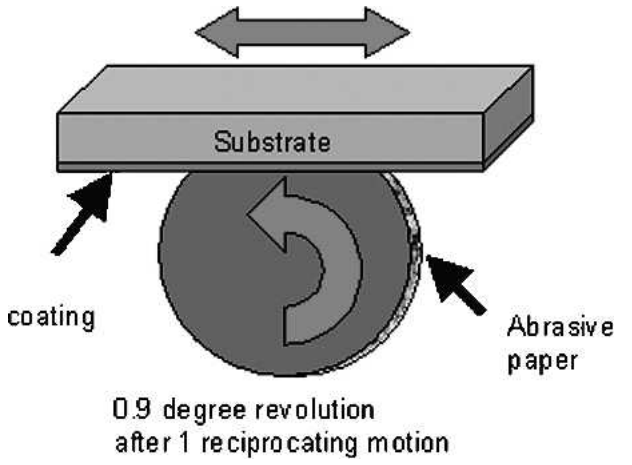

Fig. 3 Schematic representation of Suga-type wear tester; load: 30N, abrasive paper: CP240

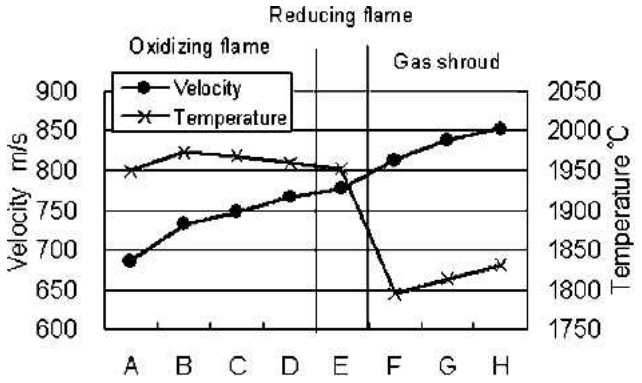

Fig. 4 Thermal spray particle's in-flight velocity and temperature under each condition

(F-H), spray particles' in-flight velocity was 800-850 m/s, and spray particles' in-flight temperature was about 1800 °C. The result shows that, by using the shroud equipment, the particle temperature dropped by 150°, whereas the particle velocity increased.

3.2 Evaluation of the Coating Structure and Properties

3.2.1 Observation of Coating Cross Sections. Typical cross sections (A, C, E, F, H) of the HVOF-sprayed coatings are shown in Fig. 5. As for the coating prepared under condition A, the coating apparently consists of deformed particles piled up on the substrate, and the boundaries among them are observed clearly. Pores and voids are visible on the cross section.

Under conditions B, C, and D, boundaries among the particles are observed revealing its lamellar structure clearly. As fuel increases from A to E, the coating's cross section gradually shows higher density. Under condition E, boundaries reveal lamellar structure slightly, and it looks like a very dense coating. Under the conditions from F to H with the gas shroud, boundaries are hardly observed, and the lamellar structure cannot be

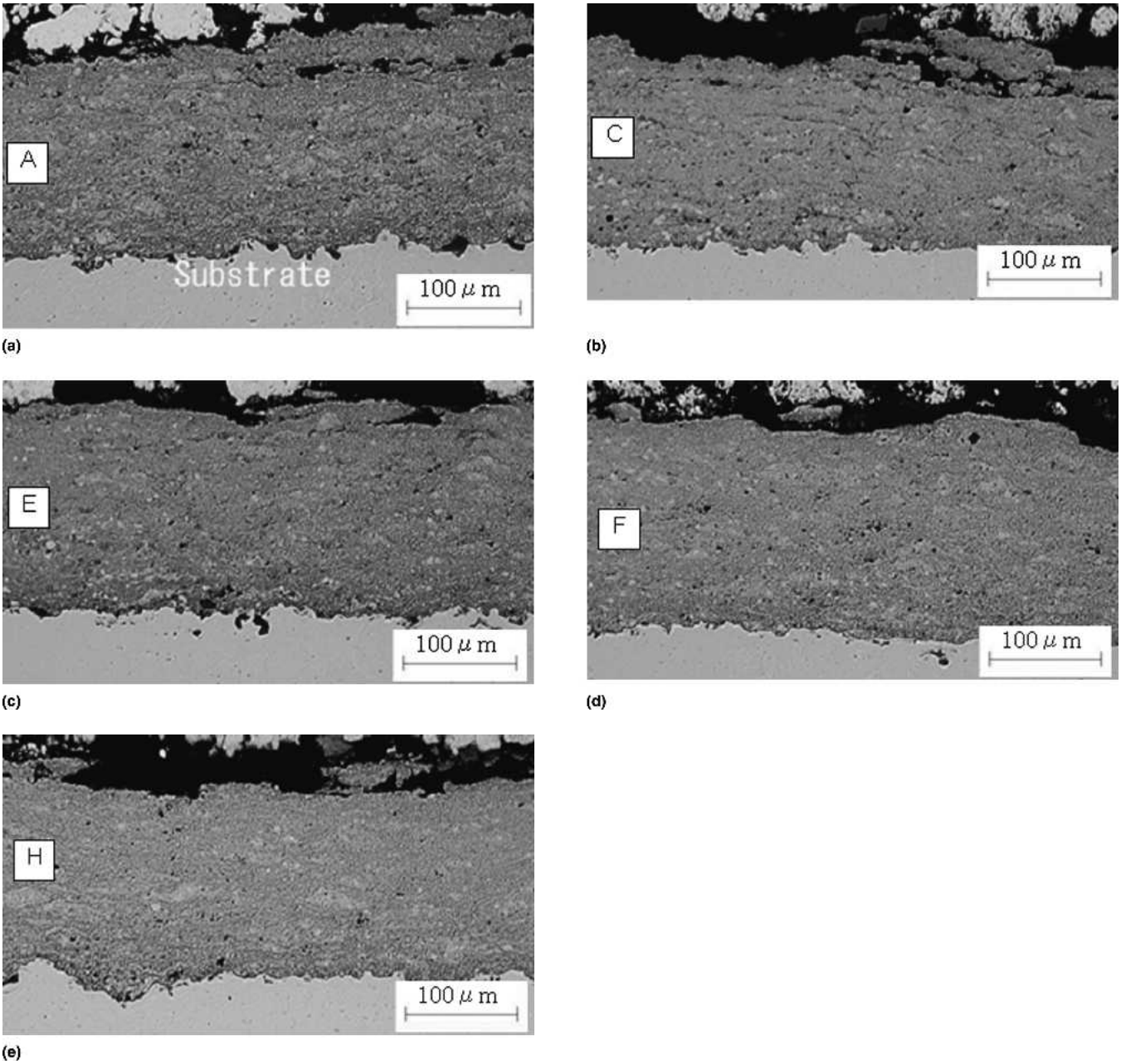

Fig. 5 Cross section of coatings under each condition

identified. This result shows the improvement in density of coating by the gas shroud attachment. Legoux et al. reported the microstructure of WC-10% Co-4% Cr coatings prepared using 4 types HVOF guns under various conditions (Ref 7). They found that the coating porosity decreased with increase of the particle velocity. This behavior is in agreement with our present observation. From A to E, with increasing the fuel/oxygen ratio, combustion pressures increased (except condition E) and spray particles' in-flight velocity increased from 680-770 m/s. However, in-flight temperature was almost fixed. Therefore, the dense structure of coating E seems to be due mainly to the effect of the high speed.

3.2.2 Corrosion Monitoring. As shown in Fig. 6, after the 72 h corrosion test, rust was generated on the coating surface under the conditions of A-D. Under the conditions of E-H, however, rust did not exist on the coating surface. Therefore, the formation of rust is likely to be related to the lower density of coatings A-D.

Figures 7 and 8 show the results of corrosion monitoring of the coatings in artificial seawater. The corrosion resistance Rc of A-D was smaller than E-H by more than an order of magnitude. The coatings E-H showed especially high corrosion resistance. The corrosion potential of A-D was −500 mV after 1.5 days. This value is equal to the corrosion potential of substrate steel (SS400), showing that through pores and voids exist in these coatings. The corrosion potential of E-H was higher than that of

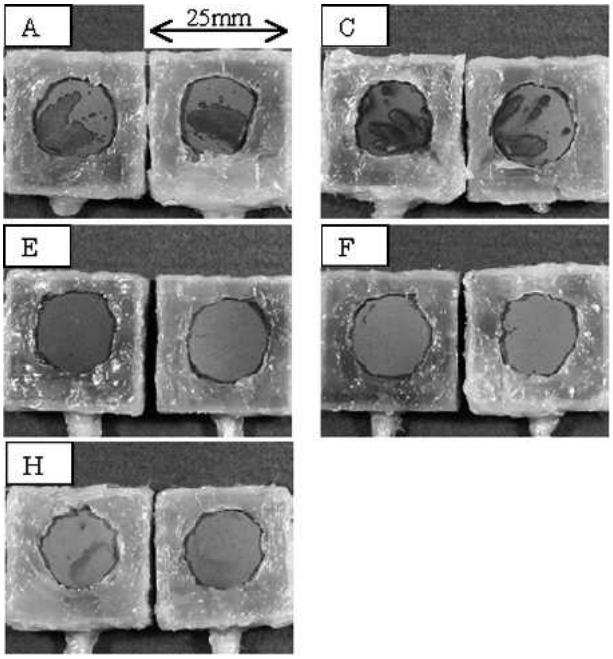

Fig. 6 Appearance of the coating surface under each condition after corrosion monitoring test

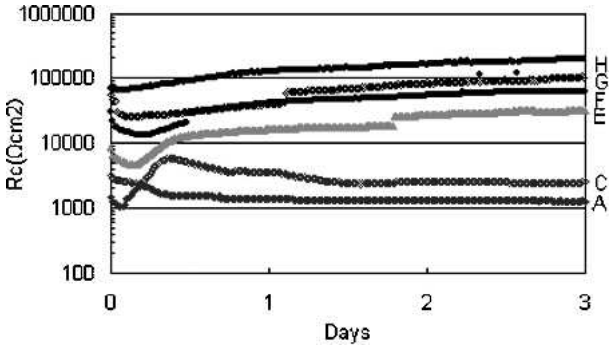

Fig. 7 Change in corrosion resistance of coatings in artificial seawater

A-D. This result suggests that the conditions of E-H produced coatings without through porosity. Harvey et al. reported that coatings characterized by denser microstructure and higher oxygen content demonstrated superior corrosion resistance (Ref 8). However, the oxygen content of the coatings should be decreased for higher corrosion and wear resistance of the coating itself. Using the gas shroud attachment, we consider that it is possible to produce dense coatings with less oxidation since the velocity of the thermal spray particles increases when the temperature of the particles is lowered.

3.2.3 X-ray Diffraction Measurement. The x-ray diffraction (XRD) diffraction spectrum of the WC/20Cr_3C_2/7Ni powder (Fig. 9) shows peaks indexed to WC, Ni, and Cr_3C_2. The XRD traces of the coatings exhibit WC and W_2C peaks along with broad diffuse peaks between $2\theta = 37$ to 46.

The ratio of W_2C-to-WC main peak heights was calculated and is shown in Fig. 10. These ratios are considered to give an indication of the degree of WC decomposition during spraying.

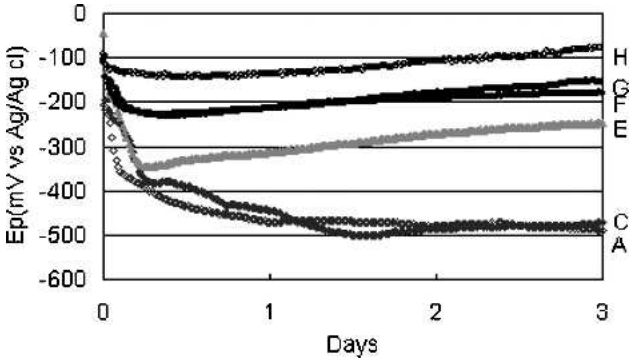

Fig. 8 Change in corrosion potential of coatings in artificial seawater

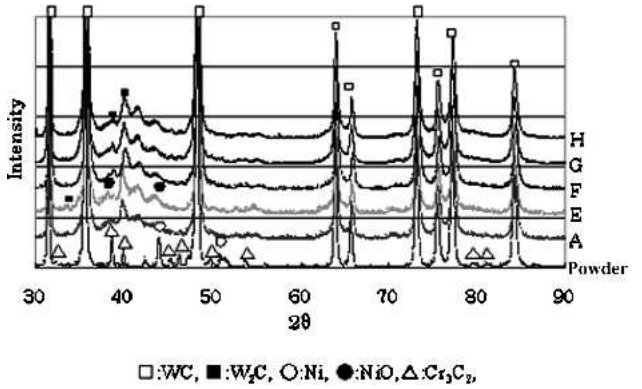

Fig. 9 XRD patterns of supply powder and coating: (□) WC, (■) W_2C, (○) Ni, (●) NiO, and (△) Cr_3C_2

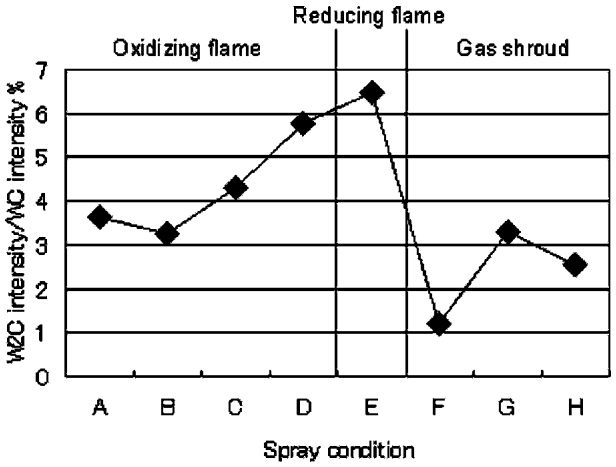

Fig. 10 Degree of WC decomposition during spraying in terms of the XRD intensity ratio of W_2C/WC

In the conventional HVOF without shroud, the W_2C intensity increased with increasing F/O ratio and reached 6.5% with the condition E, which exhibited the densest structure and highest corrosion resistance.

Bouaricha et al. reported the behavior of WC decarburization (Ref 9). The WC decarburization increased due to higher par-

ticles' temperatures. This tendency is similar to our results. With the gas shroud, higher corrosion resistance was realized with much less degree of W_2C formation.

3.2.4 Wear Properties of Coatings. Wear tests of the coatings E-H with high corrosion resistance and A were performed using the Suga type wear-tester (Fig. 11). The wear amount of the coatings F-H was smaller than that of A. The wear amount of E was between F-H and A. In the case of abrasive wear of bulk materials, it is well known that the wear amount depends on the hardness and increases linearly with testing time (Ref 10).

Figure 12 shows the result of hardness measurement on the coating cross section. Coating hardness increased with the increase of spray particle's in-flight velocity. Another fact noticed during the hardness measurement was that in all the coatings, the upper part of cross section was softer than part below.

The wear amount per rotation of the ring in the steady state in Fig. 11 is plotted against the hardness of each coating (Fig. 13). The result shows that the wear amount of the coatings is determined by the hardness of coatings.

Figure 11 also shows that initial wear amount per rotation (until measurement number 2-3) was greater than the steady state wear amount per rotation.

The change of wear rate is most likely caused by the lower hardness measured in the upper part of the coating, but another possible implication of such change in the wear rate is adhesive wear.

Adhesive wear changes from the high wear rate condition (severe wear) to the low wear rate condition (mild wear). The difference between abrasive wear and adhesive wear can be clarified from the size of wear debris.

Figure 14 shows wear debris by back scattered image (BEI). Figure 14(a) shows wear debris by the Suga type wear tester in the current study. Wear debris consists of coating's abrasive debris (white particles) and SiC abrasive grain (black particles), which dropped out from the abrasive paper. The size of the wear debris was over 10-20 μm. As a typical example of adhesive wear, the wear debris of ball-on-disk type wear test (coatings versus bearing steel ball) is shown in Figs. 14(b-1) and 14(b-2). The wear debris is very small, and the debris consists of mixture of bearing steel and coating components. From the above results, it was confirmed that the Suga type wear tester operated in the mode of abrasive wear. Therefore, the high initial wear was caused by the lower hardness of the coatings near the surface.

Because the wear mode in the real applications of such coatings is often adhesive wear, it is important to examine the severe-mild transition of the adhesive wear in the future.

4. Conclusions

A commercial HVOF and a gas shroud attachment HVOF were used to prepare WC/CrC/Ni cermet coatings under various combustion conditions (fuel/oxygen ratio, combustion pressure, introduction of inert gas to the flame by gas shroud equipment, etc.).

The density of coatings improved as the velocity of sprayed particles increased. Results of corrosion test indicate that through porosity was eliminated at the velocity above 770 m/s. GS-HVOF was effective in raising the velocity of sprayed particles by more than 50m/s whereas lowering the surface temperature by about 150K. With the conventional HVOF, the spray conditions required to achieve the high velocity resulting in higher decomposition of WC whereas with the gas shrouded HVOF, high density was achieved with a lower degree of WC degradation.

Wear resistance and hardness of the coatings prepared by GS-HVOF were superior to those prepared by the conventional HVOF.

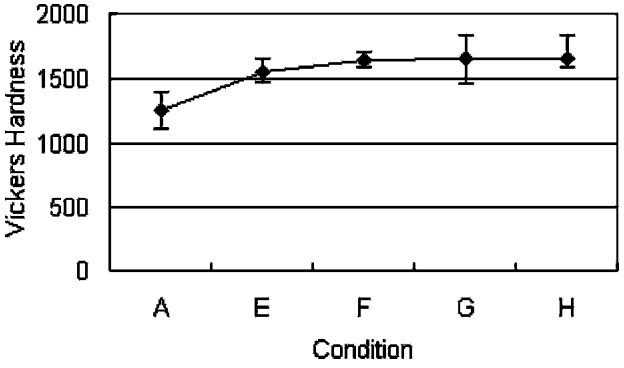

Fig. 12 Vickers hardness of coatings; indentation load: 300g The error bar shows the maximum value and minimum value.

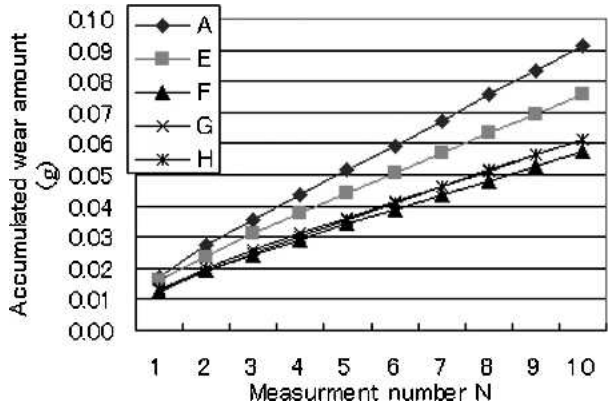

Fig. 11 Wear amount of coatings by Suga type wear tester

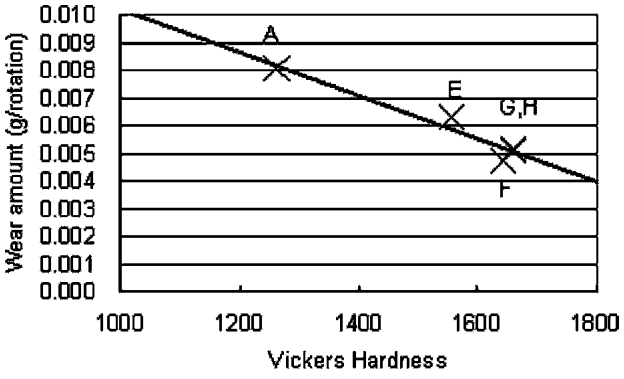

Fig. 13 Relationship between wear and hardness

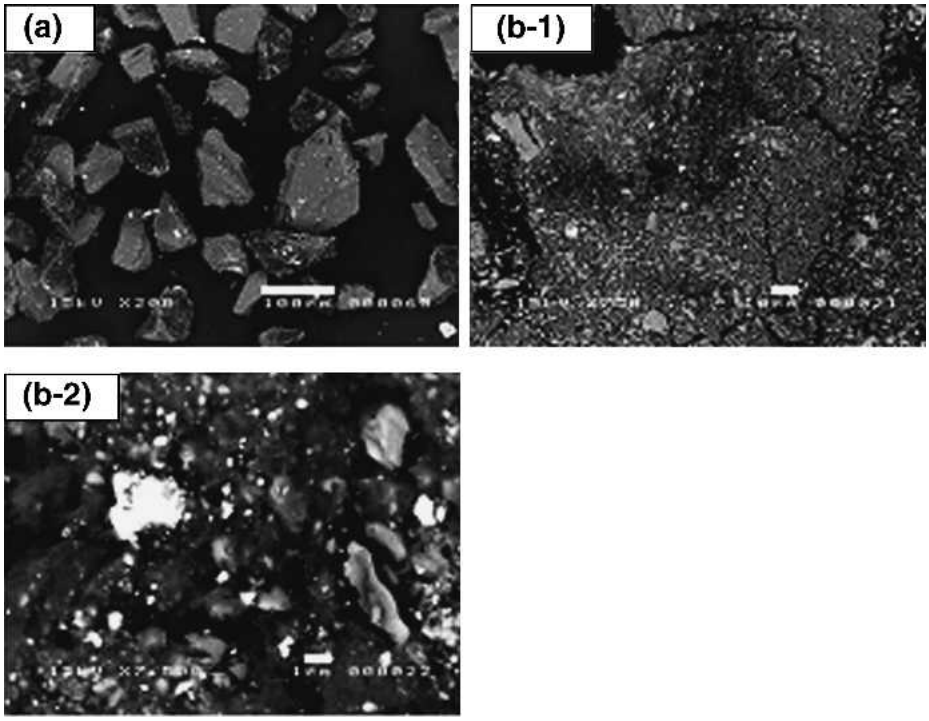

Fig. 14 BEI image of wear debris: (a) wear debris by Suga wear tester, (b) wear debris by ball on disk type tester ($WC/20Cr_3C_2/7Ni$ versus bearing steel ball); white area: WC

References

1. B. Sartwell, K. Legg, and J. Sauer, Joint Test Report, Validation of WC/Co HVOF Thermal Spray Coatings as a Replacement for Hard Chrome Plating On Aircraft Landing Gear, Part I: Materials Testing, U.S. Department of Defense, USA, 2002.
2. J.G. Legoux, Replacement of Hard Chromium Electroplating Using HVOF Thermal Spray Technology, *Proc. 7th Workshop on the Ultra-Steel,* 2003, p 124-133
3. S. Kuroda, T. Fukushima, M. Sasaki, and T. Kodama, Microstructure and Corrosion Resistance of HVOF Sprayed 316L Stainless Steel and Ni Base Alloy Coatings, *Thermal Spray: Surface Engineering via Applied Research,* C.C. Berndt, Ed., ASM International, OH, 2000, p 455-462
4. W.D. Swank, J.R. Fincke, and D.C. Haggard, HVOF Particle Flow Field Characteristics, *Thermal Spray Industrial Application,* C.C. Berndt and S. Sampath, Ed., ASM International, 1994, p 319-324
5. H. Yamada, S. Kuroda, T. Fukushima, and H. Yumoto, Capture and Evaluation of HVOF Thermal Sprayed Particles by a Gel Target, *Thermal Spray 2001: New Surface for a New Millennium,* C.C. Berndt, K.A. Khor, and E.F. Lugscheider, Ed., ASM International, 2001, p 797-803
6. T. Fukushima and S. Kuroda, Oxidation of HVOF Sprayed Alloy Coatings and Its Control by a Gas Shroud, *Thermal Spray 2001: New Surface for a New Millennium,* C.C. Berndt, K.A. Khor, and E.F. Lugscheider, Ed., ASM International, 2001, p 527-532
7. J.G. Legoux, B. Arsenault, L. Leblanc, V. Bouyer, and C. Moreau, Evaluation of Four High Velocity Thermal Spray Guns Using WC-10%Co-4%Cr Cermet, *J. Therm. Spray Technol,* Vol 11 (No. 1) 2002, p 86-94
8. D. Harvey, O. Lunder, and R. Henriksen, The Development of Corrosion Resistant Coatings by HVOF Spraying, *Thermal Spray: Surface Engineering via Applied Research,* C.C. Berndt, Ed., ASM International, Materials 2000, p 991-997
9. S. Bouaricha and B.R. Marple, Phase Structure-Mechanical Property Relationships in HVOF-sprayed WC-12Co, *Thermal Spray Solutions: Advances in Technology and Application,* DVS (Org)
10. H. Czichoz, *Tribology,* Elsevier Scientific Publishing Co., 1978, p 115